

Microstructure and tensile properties of ODS ferritic steels mechanically alloyed with Fe₂Y



J. Macías-Delgado^{a,*}, T. Leguey^a, V. de Castro^a, M.A. Auger^b, M.A. Monge^a, P. Spätig^c, N. Baluc^d, R. Pareja^a

^a Departamento de Física, Universidad Carlos III de Madrid, 28911 Leganés, Spain

^b Department of Materials, University of Oxford, Oxford OX1 3PH, United Kingdom

^c Laboratory for Nuclear Materials-NES, 5232 Villigen PSI, Switzerland

^d CRPP-EPFL, 5232 Villigen PSI, Switzerland

ARTICLE INFO

Article history:

Available online 14 October 2016

Keywords:

Oxide dispersion strengthened steels

Nanoparticles

Transmission electron microscopy

Mechanical properties

Fe₂Y

ABSTRACT

An oxide dispersion strengthened ODS ferritic steel has been produced by mechanical alloying of Fe–14Cr–2W–0.2Ti (wt.%) prealloyed powder with 0.55 (wt.%) Fe₂Y intermetallic particles and consolidated by hot isostatic pressing. The microstructure after thermal treatments confirms the homogeneous precipitation of Y–Ti oxides with nanometric sizes. Tensile properties as a function of the testing temperature from room temperature to 973 K have been measured and the results are discussed with respect to similar ODS ferritic steels fabricated by a powder metallurgy route using Y₂O₃ powder.

© 2016 The Authors. Published by Elsevier Ltd.

This is an open access article under the CC BY-NC-ND license (<http://creativecommons.org/licenses/by-nc-nd/4.0/>).

1. Introduction

Oxide dispersion strengthened (ODS) reduced activation ferritic steels having Cr contents of ~14 wt.% are one of the leading candidates for structural components of the first wall and blanket of future fusion reactors [1]. In the case of ODS Ti-modified steels, it has been found that the (Y+Ti)-rich oxide dispersion formed is finer than the Y-rich dispersion induced in a Ti free steel [2]. ODS steels have better creep resistance and superior radiation resistance than their non-reinforced counterparts, but suffer from poor toughness [3]. It is therefore vital to optimise the microstructure of ODS steels to achieve an improved mechanical behaviour and ensure their feasibility in the reactor environment. It has been found that the use of intermetallic Fe₂Y as oxide dispersion precursor instead of Y₂O₃ is effective to adjust the oxygen content in 9Cr-ODS martensitic steels [4]. In addition, it can also considerably enhance the impact properties of ODS ferritic steels [5]. However, there exists little information about the Fe₂Y effect on the microstructure and tensile properties of these materials at high temperatures.

The aim of this work is the characterization of the microstructure and mechanical properties of an ODS ferritic steel in which

the oxide dispersion has been obtained by addition of iron-yttrium intermetallic compound (Fe₂Y). Microstructural characteristics and tensile properties as a function of temperature have been obtained, and the results are discussed with respect to similar ODS ferritic steels produced using Y₂O₃ as starting powders [5–9].

2. Experimental

The mechanical alloying of the ODS powder was carried out in a Zoz Simoloyer CM08 attritor mill under a flowing H₂ atmosphere to minimize the oxygen intake. The starting components were atomised powders of Fe–14Cr–2W–0.3Ti and Fe₂Y (0.55 wt.%) purchased from Johnson Matthey. The atomized powder had oxygen content below 1000 ppm and a mean particle diameter of 25 μm. The milling lasted for 48 h Cycles of 45 s were performed at maximum rotational speed of 750 rpm, followed by 15 s at 380 rpm. The attritor chamber was filled with 1 kg of powder and the ball to powder ratio was 10:1.

The manipulation of the powder was carried out under an Ar atmosphere inside a glovebox. The milled powder was canned in a steel container, degassed for 24 h at 693 K in vacuum, sealed and consolidated by hot isostatic pressing (HIP) for 2 h at 1373 K and an Ar pressure of 175 MPa. After removing the container, the consolidated steel was heat treated at 1373 K for 30 min under vac-

* Corresponding author.

E-mail address: jumacias@fis.uc3m.es (J. Macías-Delgado).

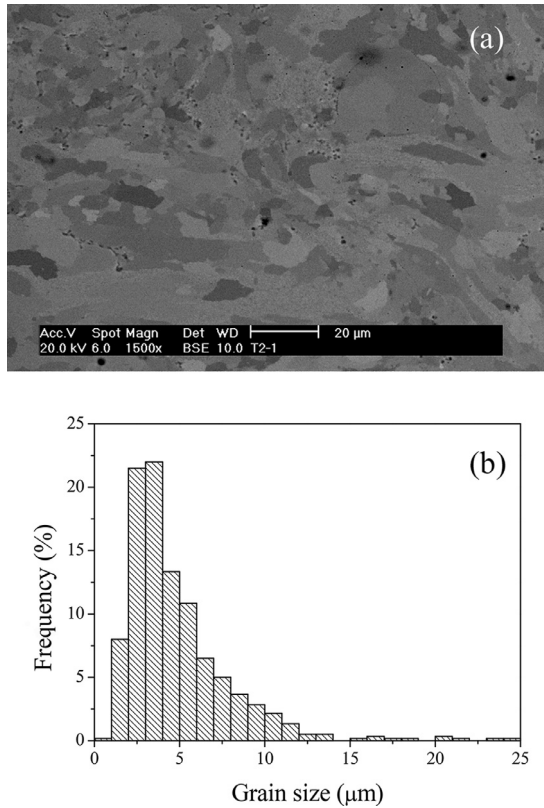


Fig. 1. (a) SEM image and (b) size distribution of grains of the Fe₂Y-ODS alloy after heat treatment.

uum, air cooled, and further heat treated at 1123 K for 2 h and air cooled. Finally, samples for microstructural analyses and mechanical characterization were cut, grinded and polished. Flat samples with gauge dimensions of $15 \times 3 \times 1 \text{ mm}^3$ were spark machined from the billet to study the mechanical properties.

The microstructure was characterized by scanning and transmission electron microscopies (SEM and TEM). SEM analyses were made using a Philips XL30 microscope equipped with an X-ray energy dispersive spectrometer (XEDS). The transmission electron microscopy was accomplished on a JEOL 3000F microscope operated at 300 keV. The ODS steel was analyzed using bright field TEM and high-angle annular dark field (HAADF) scanning (S)TEM combined with XEDS. Vickers microhardness was measured using an applied load of 300 g for 15 s. Tensile tests in the temperature range 298–973 K at a constant crosshead rate of 0.1 mm/min were performed on flat tensile specimens. Above room temperature, the tests were performed with the specimens under a flow of pure Ar to minimize the surface oxidation.

3. Results and discussion

3.1. Microstructure

The chemical composition of the milled Fe₂Y-ODS powder is shown in Table 1. The analysis shows a slight decrease of the alloy constituents (Cr, W, Ti, Y) with respect to the nominal composition. While the content of (C, N) impurities remains on a similar level, the oxygen present in the powder is 0.14%, considerably higher than the oxygen present in powders with the same composition mechanically alloyed for 20 h in a planetary ball mill, (Fe₂Y-ODS-EPFL) [5]. This effect is probably due to the type of mill used, grinding media and the longer milling time. In any case, the oxy-

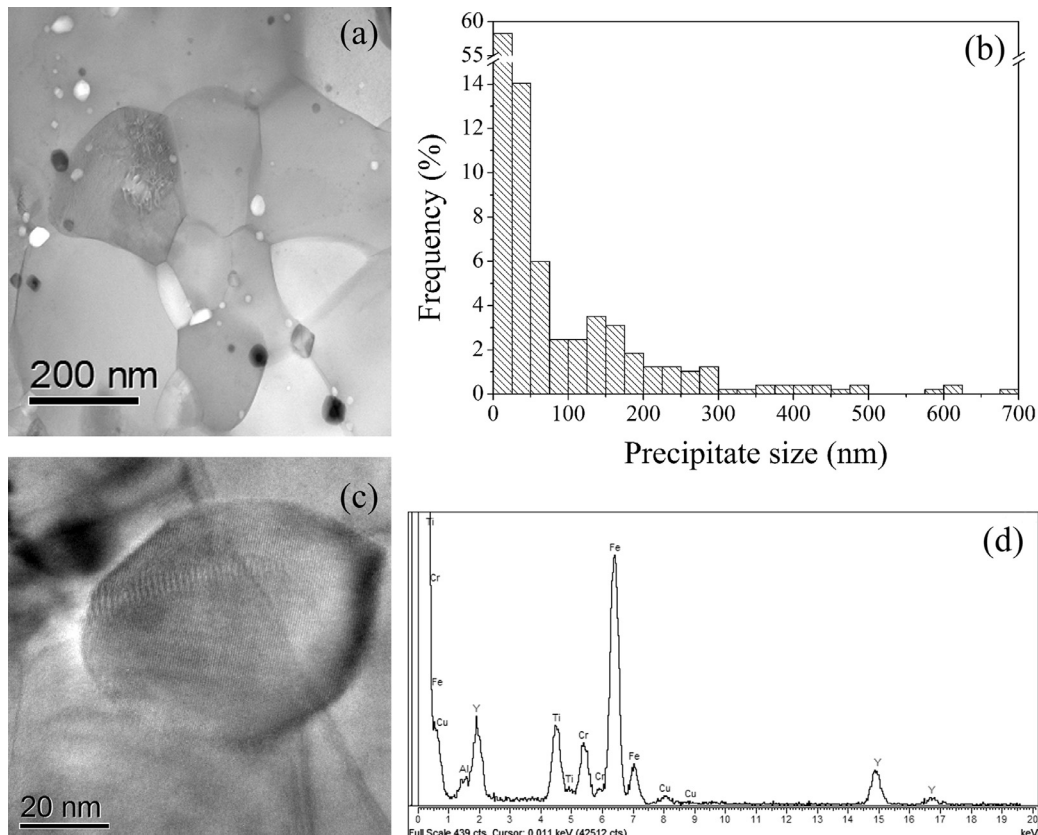


Fig. 2. (a) BF TEM image of the Fe₂Y-ODS steel after heat treatment. (b) Size distribution of the secondary phases. (c) BF image of a Y-Ti-rich precipitate. (d) XEDS point analysis of the Y-Ti-rich precipitate shown in (c), Cu signal comes from holder.

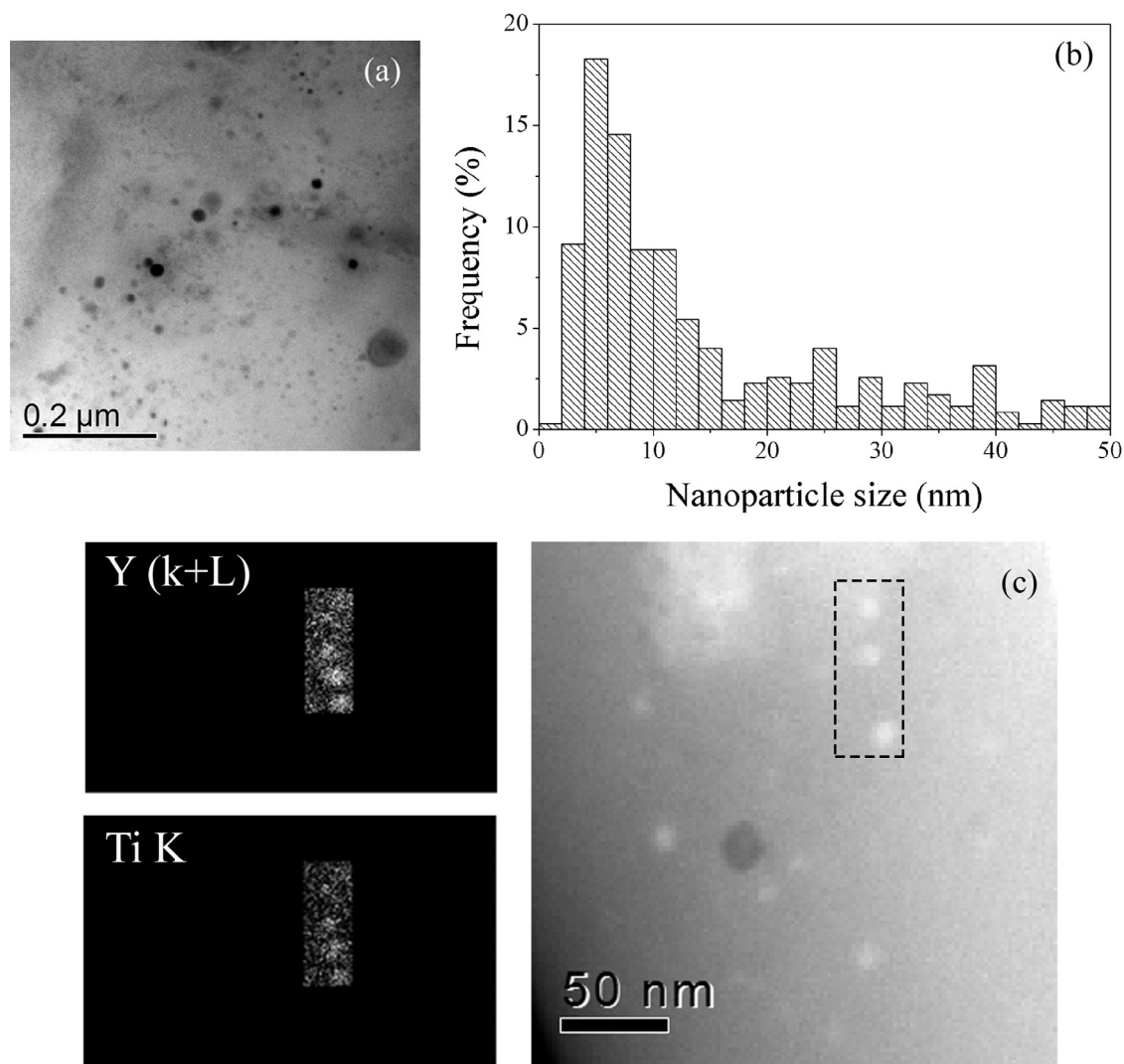


Fig. 3. (a) BF TEM image showing the dispersion of nanoparticles (b) Size distribution of the nanoparticles. (c) XEDS maps of the nanoparticles in the highlighted region.

gen content is kept lower than that reported by Oksiuta et al. in the ODS powder produced by mechanical alloying with Y_2O_3 powder [5]. Density measurement was performed on the alloy after the heat-treatment using a He ultrapycnometer. The obtained value was $7.80 \pm 0.01 \text{ g/cm}^3$. Therefore, an almost fully dense specimen, 99.73% of theoretical density ($T_d = 7.82 \text{ g/cm}^3$), was obtained.

Fig. 1 shows the microstructure of the Fe_2Y -ODS steel after the heat treatments. The general microstructure consists of equiaxed and elongated grains with sizes ranging from 1 to 25 μm. Some regions with non-recrystallized grains are also observed. These regions have already been reported for ODS steels after different thermomechanical treatments [7,8]. The grain size distribution histograms can be seen in Fig. 1b. The average grain size is $5 \pm 3 \mu\text{m}$.

Secondary phases are present in the alloy, as shown in Fig. 2a. The size distribution (~500 particles measured) is depicted in Fig. 2b, where two different populations are distinguished: small nanoparticles with sizes $\leq 50 \text{ nm}$ and larger precipitates with sizes up to 700 nm. The large precipitates are usually found close to or aligned along the grain boundaries. Their chemical composition was determined using XEDS. The precipitates analyzed were Y-Ti-rich, Ti-rich, and larger Cr-W-rich inclusions. In some precipitates the presence of Al could also be detected, although the total con-

tent of aluminum in this material is lower than 0.05 wt.%. Fig. 2c and d shows a BF image of one of those Y-Ti-rich precipitates and its corresponding XEDS analysis.

Nanoparticles with sizes between ~2 and 50 nm are found homogeneously distributed in the matrix, as Fig. 3a reveals. The nanoparticle size histogram depicted in Fig. 3b shows that most of these nanoparticles are sized between ~2 and 10 nm, with a mean value of $15 \pm 12 \text{ nm}$. Their number density was measured in regions having volumes of the order of 10^{-21} m^3 . Densities are of the order of 10^{22} m^{-3} , ranging between (1.6 ± 0.3) and $(5.9 \pm 1.2) \times 10^{22} \text{ m}^{-3}$. These values are in general similar than the ones reported for other ODS 14Cr steels produced using Y_2O_3 instead of Fe_2Y powders [6, 10]. Their chemical analysis revealed that the smallest particles ($< 15 \text{ nm}$) were Y-Ti-rich, while particles with intermediate sizes (15–50 nm) were Y-Ti-rich, Y-rich and in some cases Y-Al-rich particles. Fig. 3c shows a HAADF-STEM image of Y-Ti-rich nanoparticles and the corresponding XEDS elemental maps.

Small nanoparticles could be identified as Y-Ti oxides. Fig. 4a shows a HRTEM image of some of these Y-Ti-rich nanoparticles. The FFT image shown in the inset is in agreement with the simulated $[1\bar{2}3]$ zone pattern of the $\text{Y}_2\text{Ti}_2\text{O}_7$ structure. The corresponding XEDS point analysis is also shown in Fig. 4b. These results con-

Table 1
Chemical composition (wt.%) of the ODS steel powder after milling.

Powder	Cr	W	Ti	Y	Al	Si	O	C	S	N
Fe ₂ Y-ODS	13.0	1.6	0.15	0.20	< 0.05	<0.05	0.14	0.052	0.005	0.006
Fe ₂ Y-ODS-EPFL ^a	13.82	1.89	0.186	0.22			0.094	0.057		

^a From reference [5].

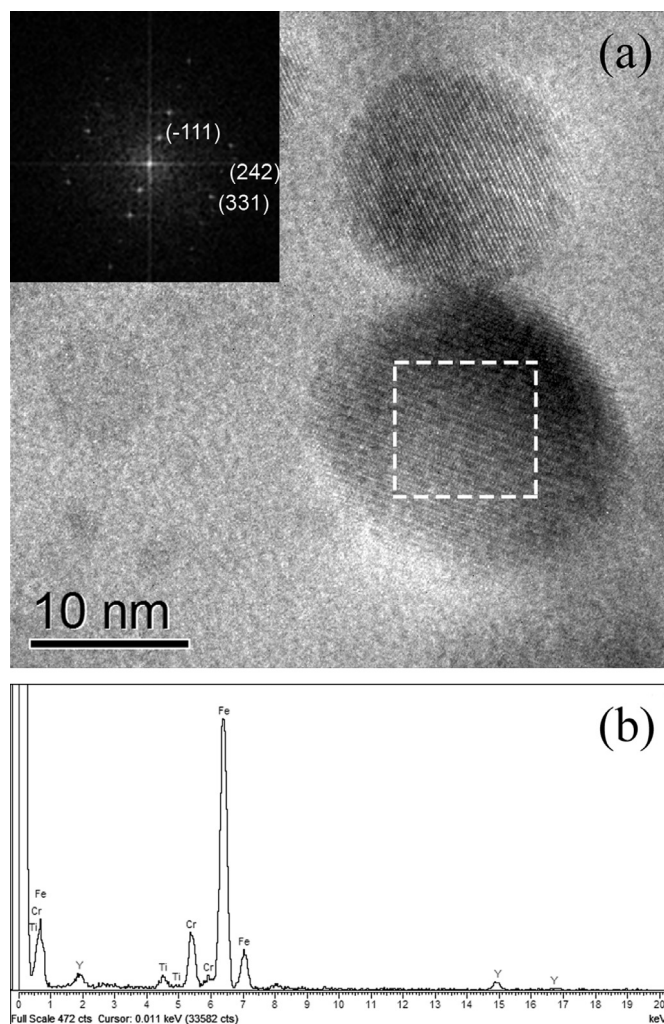


Fig. 4. (a) HREM image of Y-Ti-rich nanoparticles indexed as $Y_2Ti_2O_7$. The inset shows the indexed FFT diffractogram in zone axis $[1\ 2\ 3]$; (b) XEDS point analysis.

firm the dissolution of the intermetallic Fe_2Y and precipitation of the Y-Ti oxides during the mechanical alloying process and subsequent consolidation, as it happened with batches produced via different routes [9].

3.2. Mechanical properties

Vickers microhardness values of the consolidated material after the different heat treatments are shown in Table 2. The softening effect of the heat treatments can be seen, as the microhardness values decreases from 380 HV in the as-HIP state to 340 HV. This value is still higher than the one reported for the Fe_2Y -ODS-EPFL steel [5], although lower than the measured microhardness for the Y_2O_3 -ODS steel after forging and subsequent thermal treatments [6]. They correlate quite well with the different oxygen amount present in the compared ODS alloys.

Table 2
Microhardness of ODS steels after different heat and/or thermomechanical treatments.

Steel	Treatment	HV
Fe ₂ Y-ODS	As-HIP	380
Fe ₂ Y-ODS	HT(1373 K)	360
Fe ₂ Y-ODS	HT(1373 K)+ HT(1123 K)	340
Fe ₂ Y-ODS-EPFL ^a	As-HIP	260
Y_2O_3 -ODS ^b	F+HT(1123 K)	380

^a Ref. [5].

^{***b} Ref. [6]. HT: heat treatment, F: forging at 1423 K.

The tensile properties as a function of the testing temperature are summarized in Fig. 5, where the results obtained for the Fe_2Y -ODS steel are compared with the values reported for the Y_2O_3 -ODS steel [6]. The yield strength and tensile strength values are very similar for both materials for the whole temperature range studied, decreasing continuously with increasing temperature. The uniform and total elongation values are lower than the values obtained for the Y_2O_3 -ODS steel over the whole temperature range studied, although this effect may be due to the difference in gage length. For both alloys there is a maximum in the elongation values at ~ 773 K. This peak is characteristic of ODS ferritic steels and has been attributed with a change in the deformation mechanisms induced by the temperature [11]. At higher temperatures there is a remarkable decrease of the elongation values in the Fe_2Y -ODS alloy. The hardening ratio, defined as the tensile strength/yield strength, is also lower over the whole temperature range.

Fig. 6 shows SEM images of the fracture zone for samples tensile tested at RT, 773 K and 973 K. Fractographs show microvoid coalescence and transgranular fracture, together with flat fracture regions. Dimples are more evident in samples tested at 773 K, while more cleavage is observed at higher temperatures, with decohesion along the grain boundaries.

The results indicate that in the Fe_2Y -ODS steel, a loss of ductility at high temperatures appears in the HIP+HT condition. In order to improve the mechanical behaviour of the consolidated alloy, the grain size and grain boundary characteristics need to be modified through appropriate thermomechanical treatments such as hot forging or cross-rolling.

4. Conclusions

An ODS ferritic steel has been produced with addition of Fe_2Y as a precursor of the oxide dispersion. The microstructure of the consolidated and heat treated material reveals the complete dissolution of the intermetallic phase and formation of nanometric Y-Ti oxides homogeneously distributed in the matrix. Larger precipitates (Y-Ti-rich and Ti-rich) were also found.

The yield strength and tensile stress obtained through the whole temperature range is similar for the Fe_2Y -ODS and Y_2O_3 -ODS steels. However, the Fe_2Y -ODS steel shows lower ductility at high temperatures. An appropriate thermomechanical treatment appears to be required in order to improve the mechanical behavior at high temperatures.

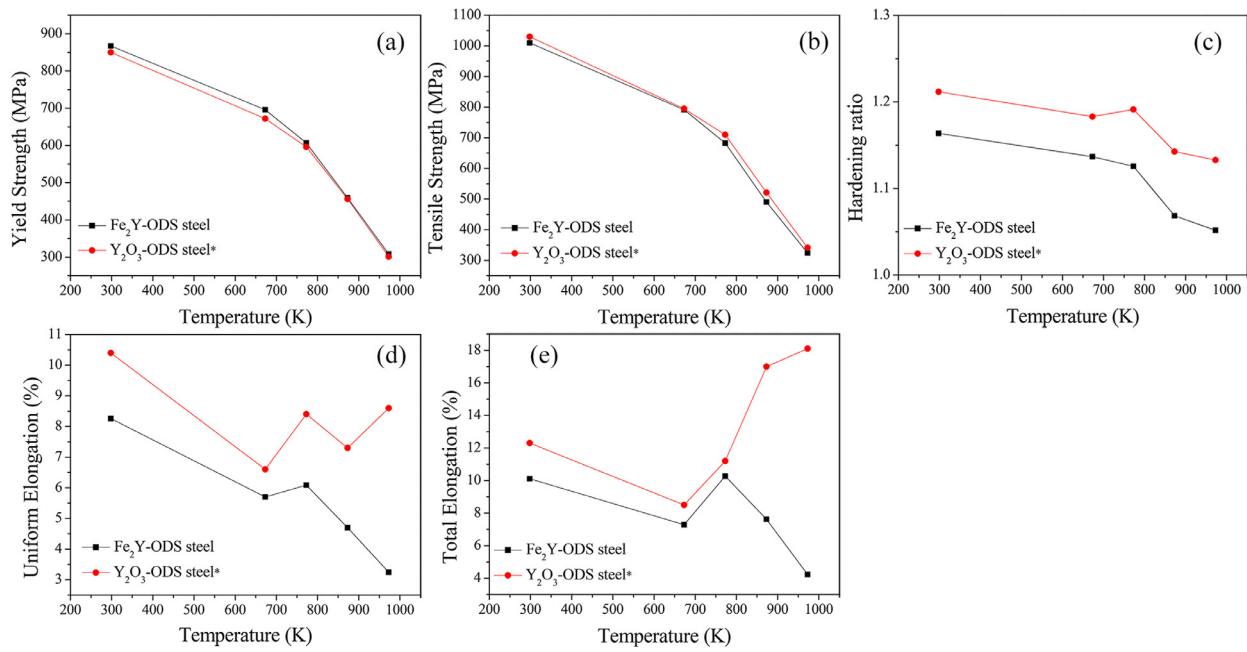


Fig. 5. Tensile properties as a function of temperature for the Fe₂Y-ODS and Y₂O₃-ODS steels. (a) Yield Strength; (b) tensile strength; (c) hardening ratio; (d) uniform elongation and (e) total elongation. * Ref. [6].

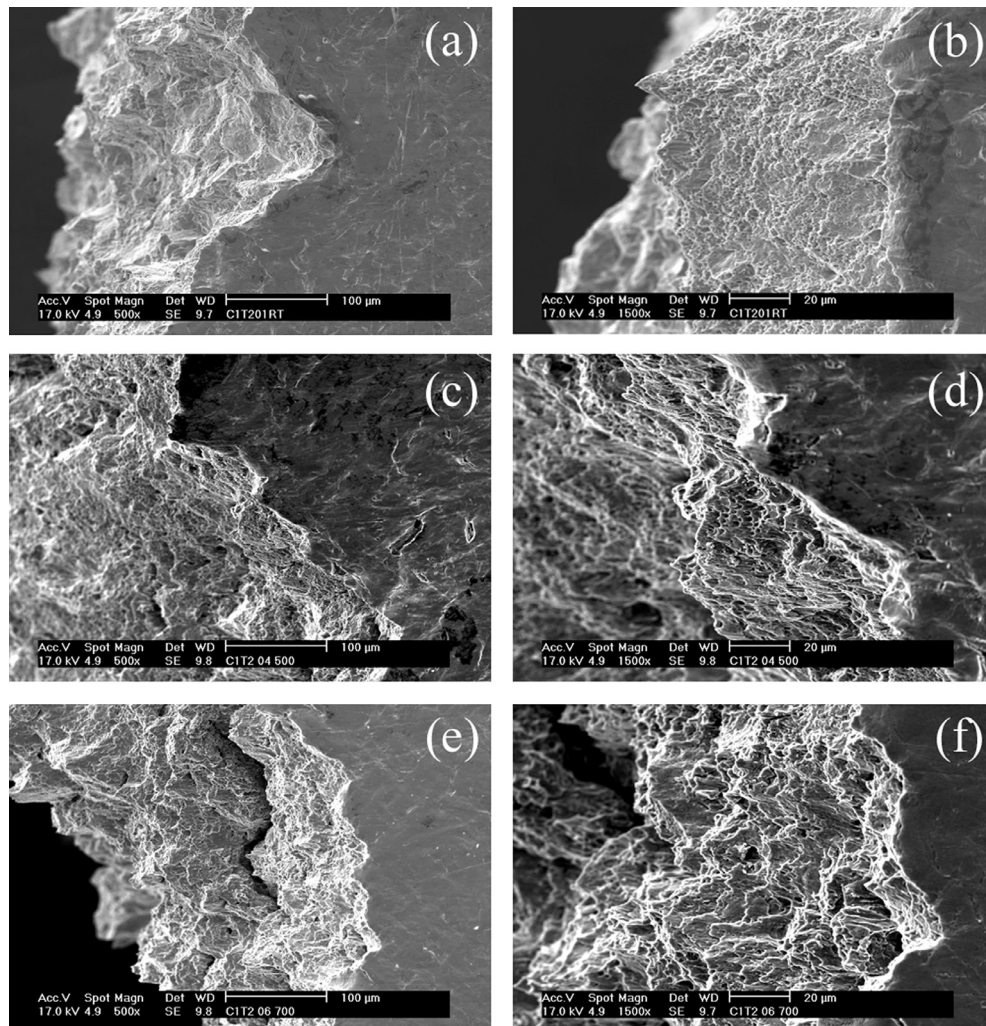


Fig. 6. SEM fractographs taken at different magnification of Fe₂Y-ODS steel tensile tested at (a, b) Room temperature, (c, d) 773 K and (e, f) 973 K.

Acknowledgements

This investigation was supported by the [Ministerio de Economía y Competitividad](#) (project [ENE2015-70300-C3-2-R](#)), the [Comunidad de Madrid](#) through the programs MULTIMAT ([S2013/MIT-2862](#)), the [European Commission](#) (EFDA) and the [European Union Seventh Framework Programme](#) under Grant Agreement [312483-ESTEEM2](#) (Integrated Infrastructure Initiative-I3). The authors also acknowledge scientific and technological advice from the Department of Materials at the University of Oxford.

References

- [1] R.L. Klueh, J. Nucl. Mater. 378 (2008) 159–166.
- [2] S. Ukai, M. Fujiwara, J. Nucl. Mater. 307–311 (2002) 749–757.
- [3] G.R. Odette, M.J. Alinger, B.D. Wirth, Annu. Rev. Mater. Res. 38 (2008) 471–503.
- [4] S. Ohtsuka, S. Ukai, M. Fujiwara, T. Kaito, T. Narita, J. Nucl. Mater. 329–333 (2004) 372–376.
- [5] Z. Oksiuta, M. Lewandowska, P. Unifantowicz, N. Baluc, K.J. Kurzydowski, Fusion Eng. Des. 86 (2011) 2417–2420.
- [6] M.A. Auger, V. de Castro, T. Leguey, M.A. Monge, A. Muñoz, R. Pareja, J. Nucl. Mater. 442 (2013) S142–S147.
- [7] V. de Castro, E.A. Marquis, S. Lozano-Perez, R. Pareja, M.L. Jenkins, Acta. Mater. 59 (2011) 3927–3936.
- [8] M.A. Auger, T. Leguey, A. Muñoz, M.A. Monge, V. de Castro, P. Fernández, G. Garcés, R. Pareja, J. Nucl. Mater. 417 (2011) 213–216.
- [9] C.A. Williams, P. Unifantowicz, N. Baluc, G.D.W. Smith, E.A. Marquis, Acta. Mater. 61 (2013) 2219–2235.
- [10] M.A. Auger, V. de Castro, T. Leguey, S. Lozano-Perez, P.A.J. Bagot, M.P. Moody, S.G. Roberts, Mater. Sci. Eng. A 671 (2016) 264–274.
- [11] M. Praud, F. Momprou, J. Malaplate, D. Caillard, J. Garnier, A. Steckmeyer, B. Fournier, J. Nucl. Mater. 428 (2012) 90–97.